

Fusion of time of arrival and time difference of arrival for ultra-wideband indoor localization

Juri Sidorenko ^{ab*}, Volker Schatz^a,
Norbert Scherer-Negenborn ^a, Michael Arens ^a,
Urs Hugentobler ^b

^aFraunhofer Institute of Optronics, System Technologies and Image Exploitation IOSB, Germany - juri.sidorenko@iosb.fraunhofer.de

^bInstitute of Astronomical and Physical Geodesy, Technical University of Munich, Germany - urs.hugentobler@tum.de

Keywords: time of arrival, time difference of arrival, localization, positioning, navigation, two-way ranging, Decawave, TWR, TOA, TDOA

1 Abstract

This article presents a new approach for the wireless clock synchronization of Decawave ultra-wideband transceivers based on the time difference of arrival. The presented techniques combine the time-of-arrival and time-difference-of-arrival measurements without losing the advantages of each approach. The precision and accuracy of the distances measured by the Decawave devices depends on three effects: signal power, clock drift, and uncertainty in the hardware delay. This article shows how all three effects may be compensated with both measurement techniques.

2 Introduction

Localization systems have become indispensable for everyday life. Satellite navigation [1, 2] has displaced paper maps and is now essential for the autonomous operation of cars and airplanes. As the requirements of logistics and manufacturing processes increase, access to precise positional information is becoming a necessity. Depending on the operating conditions for the localization application, different measurement principles [3, 4, 5] and techniques [6, 7, 8] are available. Two of the most common measurement techniques are based on the time of arrival (TOA) [6] and the time difference of arrival (TDOA) [7]. TOA calculates the distance between two stations from the signal traveling time, whereas TDOA considers the travel time differences between the stations.

Two-way ranging (TWR) uses TOA to calculate the distance between two stations [9]. In contrast to the one-way ranging approach used by satellite-based applications, the TWR approach includes a response to the transmitted signal. As a result, the transmitting stations are not required to be synchronous. In applications where not just the distance but also the position of the target (Tag) with respect to the other stations (Anchors) needs to be known, TWR is less suitable due to its slow update rate. Trilateration in two-dimensional space requires at least three distance measurements. As the number of tags increases, the update rate decreases. In contrast to TOA, TDOA remains suitable for applications with large numbers of tags. In TDOA applications, the anchors do not respond to the tags. Multilateration is performed by considering time stamp differences between anchors. Geometrically, TOA equations describe circles, whereas TDOA equations are hyperbolas in a two-dimensional space. Much like satellite navigation systems, which are based on TOA, the clocks of the TDOA anchors must be synchronized. This synchronization can be performed by wire [10] or with an additional station [3].

The measuring equipment is just as important as the measurement technique itself. This article focuses on indoor radio frequency (RF)-based localization systems. In general, indoor positioning applications are a challenge for RF-based localization systems. Reflections can generate interference with the main signal and lead to fading. Compared to narrowband signals, ultra-wideband (UWB) signals are more robust against fading [11, 12]. The Decawave transceiver [13] uses ultra-wideband (UWB) technology and is compliant with the IEEE802.15.4-2011 standard [14]. It supports six frequency bands with center frequencies from 3.5 GHz to 6.5 GHz and data rates of up to 6.8 Mb/s. Depending on the selected center frequency, the bandwidth ranges from 500 to 1000 MHz. Various methods for wireless TDOA clock synchronization are presented in [15, 16, 17]. One aspect shared by all of them is that they use a fixed and known time interval for the synchronization signal. In our case, the synchronization signal is part of the localization and the time interval does not need to be known. The solution presented here merges TOA and TDOA measurements to increase the number of equations without losing the specific advantages of each method. The measurements are provided by Decawave EVK1000 transceivers without additional synchronization hardware. This system can operate in indoor environments due to its ability to deal with fading. The precision and accuracy of the Decawave UWB depend primarily on three factors: the received signal power, the clock drift, and the hardware delay. In [Journal: signal power calibration], we showed how the signal power correction curve can be obtained automatically and how the clock drift can be corrected in every measurement. In the present publication, we demonstrate how to apply these corrections for TOA and TDOA localization.

Table 1: Notations used

Notations	Definition
T_i^R	Time stamp at the reference station
T_i^T	Time stamp at the tag
T_i^S	Time stamp at the anchor station
$\Delta T_{n,m}$	Difference between two time stamps $T_m - T_n$
$C_{n,m}$	Clock drift error calculated from the time stamps n and m
E_i	Time stamp error due to the signal power
A, B	Hardware delay
K	Time difference between the reference station and the tag
x_R, y_R, z_R	Position of reference station
x_S, y_S, z_S	Positions of base stations
x_T, y_T, z_T	Position of the tag
c_0	Speed of light

3 Clock drift and signal power correction

In [Journal: signal power calibration], we described how the clock drift and the signal power correction can be determined for the Decawave UWB transceivers. This section gives a short overview of the methods used. Figure 1 shows how the clock drift can be corrected with linear interpolation. The transmitting station (TX) sends three signals at times T_1, T_2 and T_3 . The clocks of the transmitter and the receiver are not synchronous. If the clocks have no drift, then both clocks have the same frequency, and the difference $\Delta T_{1,2} = T_2 - T_1$ is the same for both the transmitter and the receiver. If not, $\Delta T_{1,2}^{RX} \neq \Delta T_{1,2}^{TX}$. The same principle applies to $\Delta T_{1,3}$. If the clock of the reference station (RX) is running faster than the clock of the transmitter station TX, then $\Delta T_{1,3}^{RX} > \Delta T_{1,3}^{TX}$, and the clock drift error is equal to $C_{1,3} = \Delta T_{1,3}^{RX} - \Delta T_{1,3}^{TX}$. Using linear interpolation, we can estimate the shift of the timestamp T_2 due to clock drift. The correction term is equal to $\frac{C_{1,3}}{\Delta T_{1,3}^{TX}} \cdot \Delta T_{1,2}^{TX}$. A position error caused by a constant velocity of the object is also corrected by the linear interpolation, due to the linear increase of the position error (pseudo clock drift). In practise, is $\Delta T_{1,3}^{TX}$ about 1 ms. An acceleration high enough to cause an error greater than 5 mm, would require near most 1,000g ($10^4 \frac{m}{s^2}$). The standard approach uses the integral of the phase-locked loop (PLL) to calculate the correction value. In [Journal: signal power calibration], we showed that this correction method may not be suitable due to its dependency on the signal power. Alternative methods such as symmetric and asymmetric double-sided two-way ranging [9] do not calculate the clock drift but use three or more messages to reduce the error.

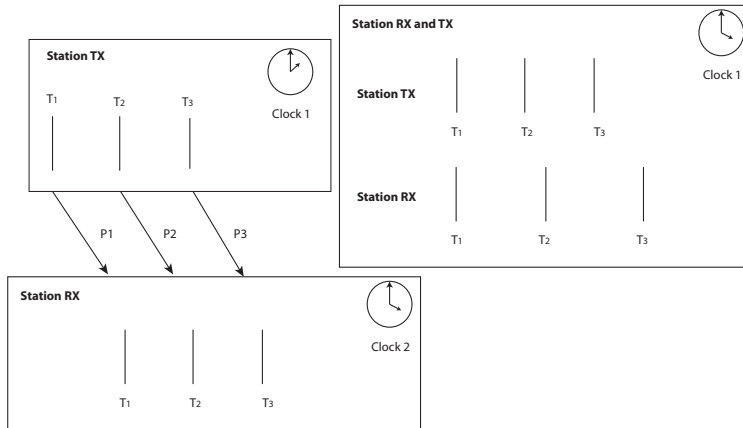


Figure 1: An alternative clock drift correction [JOURNAL: SIGNAL POWER]

The timestamp of the DW1000 is known to be affected by the signal power [18, 19]. Increasing the signal power causes a negative shift of the time stamp and vice versa. In [Journal], we showed how the signal power correction curve can be determined for each Decawave UWB transceiver individually without requiring additional measurement equipment. Figure 2 shows the correction curves for the measured vs. the actual signal power and the actual signal vs. the timestamp error.

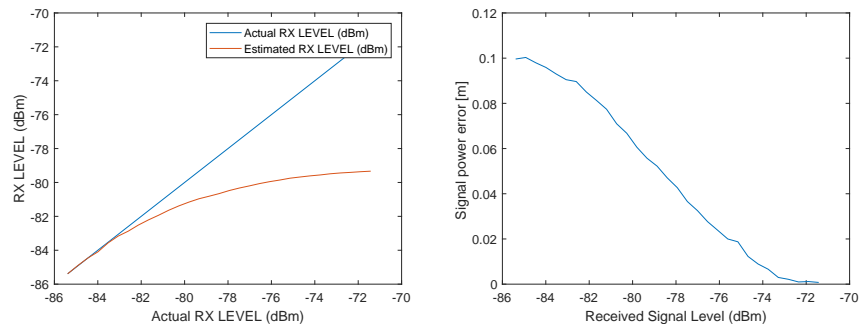


Figure 2: Final results of the power correction . Left: Measured signal power vs. real signal power. Right: Signal power error curve [JOURNAL: SIGNAL POWER]

4 Time of arrival

Figure 3 illustrates the concept of TWR and the timestamp shift caused by signal power, as well as the error due to hardware delay. In our implementation, the reference station is the initiator. The first message is sent by the reference

station with timestamp T_1^R . The timestamp of the received message at the tag is affected by the signal power, resulting in a timestamp shift of E_1 . The same applies to the response message, this time at the reference station. It is important to note that the timestamps T_1^R and T_2^T are not affected by the receiving signal power. However, the hardware delay (A,B) must always be considered. The sending delay is assumed to be equal to the receiving delay. Without correction, the TWR signal travel time is $0.5 \cdot ((T_2^R - T_1^R) - (T_2^T - T_1^T))$.

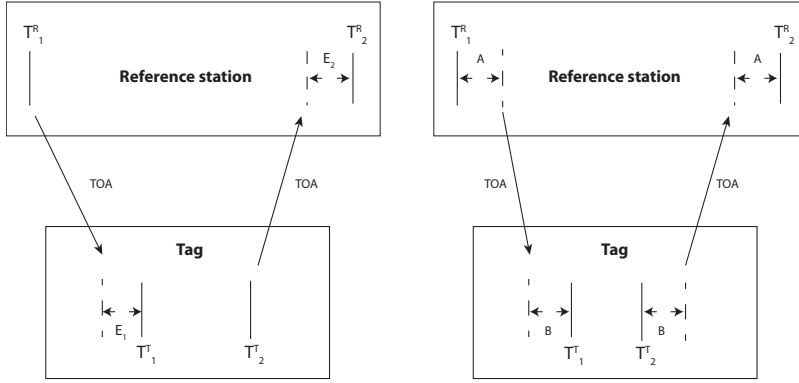


Figure 3: Left: Effect of the power on the TOA, Right: Effect of the hardware delay on TOA

The corrected time of flight between the reference station and the tag can be estimated with the following formula.

$$T_{TOA} = 0.5 \cdot ((T_2^R - T_1^R) - (T_2^T - T_1^T) - E_2 - E_1) - A - B \quad (1)$$

The values E_1 and E_2 are deduced from the signal power correction curve. Note that the signal power may affect the tag and the reference station differently. At lower signal power, the time difference $\Delta T_{1,2}^R$ increases.

In the previous section, we showed that the clock drift can be corrected by three messages. Figure 4 demonstrates how this principle can be adapted for two-way ranging. The last message is used to calculate the clock drift error $C_{1,3}^{RT} = \Delta T_{1,3}^R - \Delta T_{1,3}^T$. Observe that the signal power E_1 does not affect the timestamp difference $\Delta T_{1,3}^T$. The final time of flight equation with the clock drift correction and three messages is as follows:

$$T_{TOA} = 0.5 \cdot \left(\Delta T_{1,2}^R - \Delta T_{1,2}^T - \left(\frac{C_{1,3}^{RT}}{\Delta T_{1,3}^T} \cdot (\Delta T_{1,2}^T + E_1) \right) - E_2 - E_1 \right) - A - B \quad (2)$$

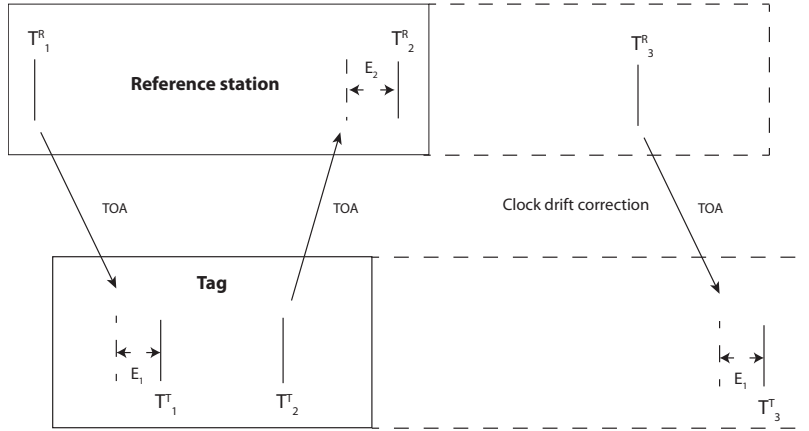


Figure 4: TWR clock drift correction

Given the corrected time measurements, the TOA, and the propagation speed of the signal, lateration may be performed to deduce the position of the tag (x_T, y_T, z_T) with respect to the anchors, by solving the following system of equations.

$$T_{TOA_i} \cdot c_0 = \sqrt{(x_{R_i} - x_T)^2 + (y_{R_i} - y_T)^2 + (z_{R_i} - z_T)^2} \quad 1 \leq i \leq N$$

5 Time difference of arrival

The previous section showed how the clock drift and the hardware offset influence the time-of-arrival position estimate. In this section, we show how to combine TOA with TDOA. Unlike TDOA, two-way ranging (TWR) based on TOA does not require clock synchronization. One approach to synchronizing the TDOA clock is to use an additional signal [3]. This signal is already present in the two-way ranging (TWR) approach, so a combination of both techniques seems natural. This principle is illustrated in figure 6. The effect of the clock drift and the hardware delay on the TDOA can be seen in figure 5. Two-way ranging is performed between the tag and the reference station. The other stations are passive and do not respond to the reference station or tag. The difference between timestamps two and one at each anchor depends on the positions of the reference station and the tag with respect to the anchor. Unlike the TWR application presented earlier, the influence of the signal power and the hardware delay differs in the TDOA application.

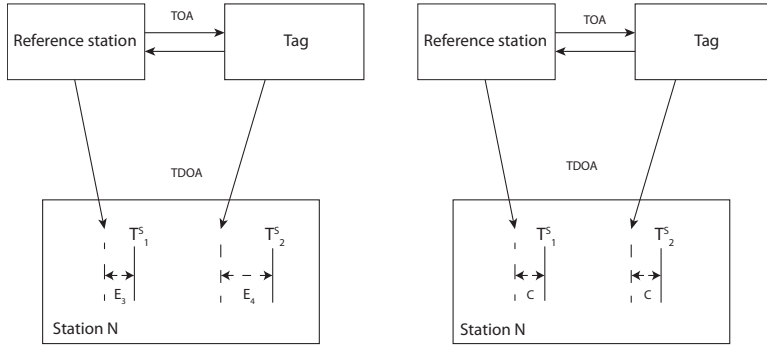


Figure 5: Left: Effect of power on the TDOA, Right: Effect of the hardware offset on the TDOA

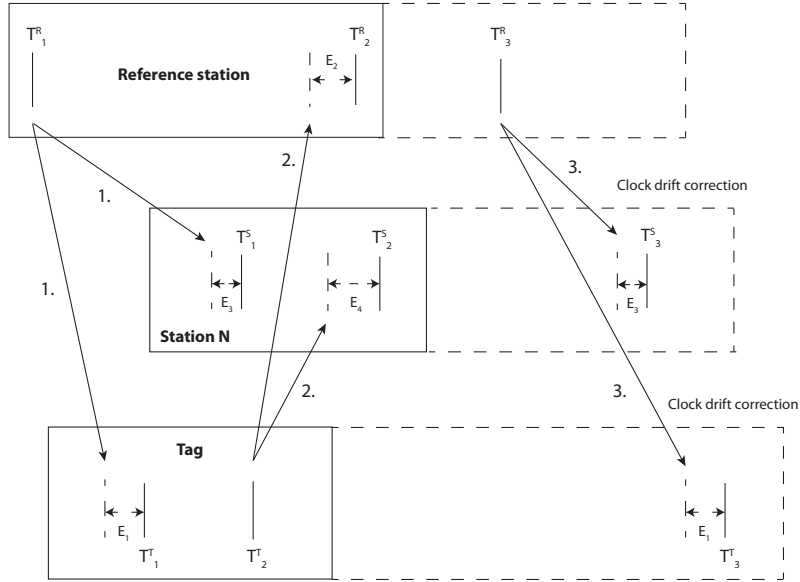


Figure 6: TOA and TDOA clock drift correction

In the TDOA application, the influence of the hardware delay is assumed to be the same for both timestamps T_1^S and T_2^S . Therefore, the TDOA equation is independent of the hardware delay. However, a new offset K appears, representing the delay between the signal of the tag with respect to the signal of the reference station. If both stations send the signal at exactly the same time, this offset K is zero.

$$T_{TDOA_K} = \Delta T_{1,2}^S - E_4 + E_3 + K \quad (3)$$

The third message from the reference station $\Delta T_{1,3}^S = T_3^S - T_1^S$ is used to calculate the clock drift error $C_{1,3}^S$.

$$C_{1,3}^S = \Delta T_{1,3}^R - \Delta T_{1,3}^S \quad (4)$$

After performing a linear interpolation of the clock drift error $C_{1,3}^S$, the TDOA equation becomes

$$T_{TDOA_K} = \Delta T_{1,2}^S + \left(\frac{C_{1,3}^S}{\Delta T_{1,3}^S} \cdot (\Delta T_{1,2}^S + E_3 - E_4) \right) - E_4 + E_3 + K \quad (5)$$

This equation still depends on the offset K. However, this offset is simply the traveling time of the signal from the reference station to the tag plus the computation time at the tag before the signal is emitted. It may be calculated as follows:

$$K = T_{TOA} + \Delta T_{1,2}^T + \left(\frac{C_{1,3}^{RT}}{\Delta T_{1,3}^T} \cdot (\Delta T_{1,2}^T + E_1) \right) + E_1 + 2B \quad (6)$$

The new TDOA equation after eliminating the offset K and including all corrections is as follows:

$$T_{TDOA} = \left(\frac{C_{1,3}^S}{\Delta T_{1,3}^S} \cdot (\Delta T_{1,2}^S + E_3 - E_4) \right) + 0.5 \left(\Delta T_{1,2}^T + \frac{C_{1,3}^{RT}}{\Delta T_{1,3}^T} \cdot (\Delta T_{1,2}^T + E_1) \right) + \Delta T_{1,2}^S + 0.5 \cdot \Delta T_{1,2}^R - A + B + 0.5(E_1 - E_2) + E_3 - E_4 \quad (7)$$

From each measurement, we can now obtain one TOA equation and multiple different TDOA equations, depending on the number of anchors. This method supports high update rates with just four stations for localization in a two-dimensional space – two anchors, one reference station, and one tag.

$$T_{TOA_1} \cdot c_0 = \sqrt{(x_{R_1} - x_T)^2 + (y_{R_1} - y_T)^2}$$

$$T_{TDOA_i} \cdot c_0 = \sqrt{(x_T - x_{S_i})^2 + (y_T - y_{S_i})^2} - \sqrt{(x_{R_1} - x_{S_i})^2 + (y_{R_1} - y_{S_i})^2}$$

$$1 \leq i \leq N$$

This equation is not symmetric due to the dependency on the noise of reference station. The reference station should therefore be selected to have the lowest possible noise. We recommend readers to refer to our previous publication on symmetric TDOA equations [20].

6 Two-dimensional position estimation with four stations

In this section, the theoretical concepts are verified with real measurements. The first test scenario uses TOA measurements to estimate the unknown position of the tag. In the second test scenario is the position of the tag estimated by the fused measurements of TDOA and TOA.

The tests were carried out with a Decawave EVB DW1000. The Decawave supports different message types, which are specified for the discovery phase, ranging phase and final data transmission. Depending on the update rate and the preamble length, each message can vary from 190 μ s to 3.4 ms. In our experiments, we only used 190 μ s messages, also called blink messages. The general settings of the Decawave transceivers are listed in table 2.

Channel	2
Center Frequency	3993.6 MHz
Bandwidth	499.2 MHz
Pulse repetition frequency	64 MHz
Preamble length	128
Data rate	6.81 Mbps

Table 2: Test settings

Figure 7 and table 3 show the constellation of the stations. The ground truth data were obtained by laser distance measurement. The position of the tag with identification number (ID) 2 is assumed to be unknown. The other stations are used to estimate the position of this tag. The station identified as the reference station changes during TWR positioning. This is because the distances between the tag and the other stations must be calculated successively for TWR trilateration. Unlike TWR, the reference station remains the same for TDOA; in this example, the reference station is the station with ID 1. This also explains why TDOA is much faster than TWR.

Station ID	X-Axis [m]	Y-Axis [m]
1	0	0
2	0	1.5134
3	1.27	1.643
4	1.1439	0.0385

Table 3: Position of the stations obtained by laser distance measurements



Figure 7: Constellation of the stations

Figure 8 shows the results of the TOA and TDOA position estimate of station 2. The mean values of TOA and TDOA differ by 0.0023 m on the x-axis and 0.0006 m on the y-axis. This difference is small, indicating that the assumptions regarding the offset and the clock drift are correct. The deviation between the mean values of the TOA and TDOA measurements and the ground truth data may be explained by uncertainty in the hardware delay and the ground truth data estimate.

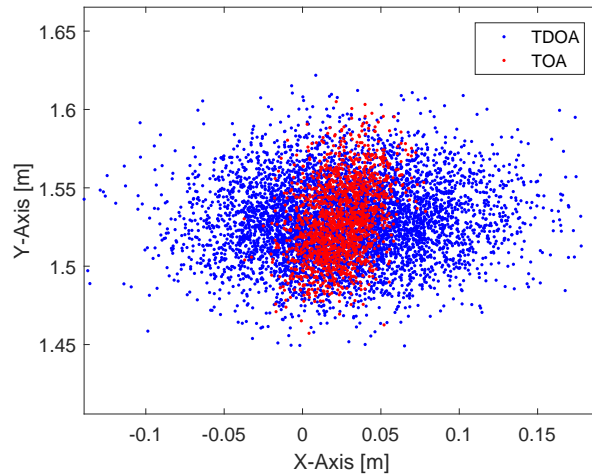


Figure 8: X/Y positions of the TOA and TDOA fused with TOA position estimates

The following table 5 shows the standard deviation of the precision of the TOA and TDOA position estimates. The y-axis scattering is almost exactly equal for both measurement techniques. On the other hand, the x-axis scattering of TDOA is higher than that of TOA, depicted in Table 4.

$$Cov(TDOA) = \begin{pmatrix} 0.0023 & 0.0001 \\ 0.0001 & 0.0007 \end{pmatrix} \quad Cov(TOA) = \begin{pmatrix} 0.0003 & 0.0001 \\ 0.0001 & 0.0006 \end{pmatrix}$$

Table 4: Covariance matrix of the TOA and fused TDOA measurements

This effect is due to the asymmetry of the TDOA, which is actually a fusion of TWR and TDOA. An alternative reference station would change the distribution. The compensation of this effect is described in a previous publication [20]. When combined with a filter, highly accurate results can be obtained. The position of the anchors affects the tag localization; better results are obtained with tags that are more centered with respect to the anchors [21].

	TOA	TDOA
X-axis [m]	0.0175	0.0479
Y-axis [m]	0.0249	0.0256

Table 5: Precision: Standard Deviation

The accuracy depends on the true position of the anchors and the offset estimate. This topic will be explained in detail in an upcoming publication.

7 Conclusion

This paper introduces a method of clock drift, signal power dependency, and hardware delay correction for measurements based on the time of arrival and the time difference of arrival. We showed how wireless clock calibration can be performed for the time difference of arrival using an additional station. The corrected time of arrival and time difference of arrival measurements were combined to increase the number of equations for the time difference of arrival position estimate. The final section of the paper examined the theoretical concepts presented in previous sections against real measurements from Decawave EVK1000 UWB transceivers.

References

- [1] D. Douglass and K. Monahan. GPS instant navigation : A practical guide from basics to advanced techniques by kevin monahan. *Fine Edge Productions*, 1998.
- [2] RB Thompson. Global positioning system: the mathematics of GPS receivers. *Mathematics magazine*, 1998.

- [3] A. Resch, R. Pfeil, M. Wegener, and A. Stelzer. Review of the lpm local positioning measurement system. In *2012 International Conference on Localization and GNSS*, pages 1–5, June 2012.
- [4] Xiaolong Shen, Shengqi Yang, Jian He, and Zhangqin Huang. Improved localization algorithm based on rssi in low power bluetooth network. In *2016 2nd International Conference on Cloud Computing and Internet of Things (CCIOT)*, pages 134–137, Oct 2016.
- [5] L. Zwirello, T. Schipper, M. Jalilvand, and T. Zwick. Realization limits of impulse-based localization system for large-scale indoor applications. *IEEE Transactions on Instrumentation and Measurement*, 64(1):39–51, Jan 2015.
- [6] David L. Adamy. *EW 102: A Second Course in Electronic Warfare*. Artech House, Boston London, 2004.
- [7] Y. Zhou, C. L. Law, Y. L. Guan, and F. Chin. Indoor elliptical localization based on asynchronous uwb range measurement. *IEEE Transactions on Instrumentation and Measurement*, 60(1):248–257, Jan 2011.
- [8] I. Dotlic, A. Connell, H. Ma, J. Clancy, and M. McLaughlin. Angle of arrival estimation using decawave dw1000 integrated circuits. In *2017 14th Workshop on Positioning, Navigation and Communications (WPNC)*, pages 1–6, Oct 2017.
- [9] B. Barua, N. Kandil, and N. Hakem. On performance study of twr uwb ranging in underground mine. In *2018 Sixth International Conference on Digital Information, Networking, and Wireless Communications (DINWC)*, pages 28–31, April 2018.
- [10] *Decawave APS007 APPLICATION NOTE: Wired synchronisation of anchor nodes in a TDOA real time location system, Version 1.0*.
- [11] J. F. M. Gerrits, J. R. Farserotu, and J. R. Long. Multipath behavior of fm-uw b signals. In *2007 IEEE International Conference on Ultra-Wideband*, pages 162–167, Sept 2007.
- [12] R. A. Saeed, S. Khatun, B. M. Ali, and M. A. Khazani. Ultra-wideband (uwb) geolocation in nlos multipath fading environments. In *2005 13th IEEE International Conference on Networks Jointly held with the 2005 IEEE 7th Malaysia International Conf on Communic*, volume 2, pages 6 pp.–, Nov 2005.
- [13] A. R. Jiménez Ruiz and F. Seco Granja. Comparing ubisense, bespoon, and decawave uwb location systems: Indoor performance analysis. *IEEE Transactions on Instrumentation and Measurement*, 66(8):2106–2117, Aug 2017.

- [14] M. Haluza and J. Vesely. Analysis of signals from the decawave trek1000 wideband positioning system using akrs system. In *2017 International Conference on Military Technologies (ICMT)*, pages 424–429, May 2017.
- [15] C. McElroy, D. Neirynek, and M. McLaughlin. Comparison of wireless clock synchronization algorithms for indoor location systems. In *2014 IEEE International Conference on Communications Workshops (ICC)*, pages 157–162, June 2014.
- [16] V. Djaja-Josko and J. Kolakowski. A new method for wireless synchronization and tdoa error reduction in uwb positioning system. In *2016 21st International Conference on Microwave, Radar and Wireless Communications (MIKON)*, pages 1–4, May 2016.
- [17] J. Tiemann, F. Eckermann, and C. Wietfeld. Atlas - an open-source tdoa-based ultra-wideband localization system. In *2016 International Conference on Indoor Positioning and Indoor Navigation (IPIN)*, pages 1–6, Oct 2016.
- [18] *DW1000 User Manual, Version 2.15, Page 45.*
- [19] *Decawave APS011 APPLICATION NOTE: Sources of error in TWR schemes, Version 1.0, Page 10.*
- [20] J. Sidorenko et al. Improved linear direct solution for asynchronous radio network localization (rnl). *Institute of Navigation ION Pacific PNT Meeting*, 2017.
- [21] N. Salman, H. K. Maheshwari, A. H. Kemp, and M. Ghogho. Effects of anchor placement on mean-crb for localization. In *2011 The 10th IFIP Annual Mediterranean Ad Hoc Networking Workshop*, pages 115–118, June 2011.